DELAY OF CATASTROPHIC BOUNDARY LAYER SEPARATION OVER NACA 23012 AIRFOIL; A NUMERICAL STUDY

Julius, M.O.[1]* and Alonge, O. I.[2]

[1] Department of Mechanical Engineering, Obafemi Awolowo University, Ile-Ife, Osun State, Nigeria.

[2] Department of Mechanical Engineering, Elizade University, Ilaramokin, Ondo State, Nigeria.

*Email of Corresponding Author: mosesjulius41@gmail.com

ABSTRACT

Flow separation is caused by the action of the combined effect of the adverse pressure gradient and viscous force on the surface of the aeroplane wing and these lead to enormous loss of energy. Consequently, the aerodynamic performance is adversely affected (i.e. there is lift reduction and drag enhancement) and may lead to a catastrophe which put the safety of the aeroplane and the lives on it in danger. The introduction of suction slots, flaps, sophisticated high lifting devices to control the flow through separation delay can mitigate the aerodynamic losses. Therefore, this paper focuses on using a perpendicular suction to control the boundary layer separation of flow over the NACA 23012 aerofoil in order to stem the stalling effect that may lead to fatality. This was achieved by careful design and optimisation of the suction positions, suction jet amplitudes and other geometric parameters. The Reynolds Average Navier-Stokes (RANS) equations were employed together with the Menter's shear stress turbulent model. The jet with of 2.5% of the chord length was placed at different position varied from 10% to 70% of the chord length; the jet velocity was varied from 0.1 to 0.3 of the free stream velocity. The result of this study demonstrated that when the jet position is moved towards the trailing edge the lift to drag ratio decreases. Also, as the jet amplitude was increased, the lift to drag ratio increased commensurately. The jet position of 0.2c and jet amplitude of 0.3 is the most effective to improve the lift to drag ratio when compared to the NACA 23012 without suction. So the point of separation is delayed and the lift is increased significantly.

Keywords: flow control, jet width, lift to drag ratio, suction, boundary layer separation, turbulent flow.

INTRODUCTION

In recent times and decade's age, most of the catastrophes on aeroplanes are caused by flow separation. The flow separation leads to loss of streamwise momentum which affects the aerodynamic performance of an aeroplane (lift enhancement, drag reduction and stall improvement) causing enormous loss of energy. At a low angle of attack, the flow over the streamline body (such as airfoil) is close to that of the inviscid theory prediction flow pattern (Snorri, 2013). However, at a high angle of attack or low Reynolds numbers, the combined action of viscous force (skin friction) and adverse pressure gradient enhances the formation of flow separation around the trailing edge which advances towards the leading edge as the angle of attack increase (Schlichting, 1955). The investigations into the boundary layer have produced numerous solutions to many design problems in areas of fluid mechanics through flow or boundary layer control. Flow control is the process of manipulating flow around a smooth straight surface to behave differently from its normal norms. The control of boundary layer separation can be grouped into two: passive method and active method. The active methods require energy expenditure while passive methods do not require energy expenditure (Gad-el_Hak, 2000). Various works of literature have considered works of literature different technique to control flow in order to delay the transition, postpone separation, enhance lift, reduce drag, suppress noise, and augment turbulence. Prandtl (Schlichting, 1955) was the first scientist to experimentally investigate flow control through the application of suction on a cylindrical surface and he revealed that boundary layer separation would be eliminated almost entirely via suction through a slot on the back of the cylinder. Jacobs and Clay (1936) experimentally studied the aerodynamic characteristics of NACA 23012 wing under various aerodynamic conditions as compared to Clark Y and other NACA's airfoils. They concluded that NACA 23012 has the best aerodynamic characteristics. The development of sophisticated computation facilities in the past few decades has resulted in an increase in the use of computational fluid dynamics to investigate boundary layer control. Various numerical works have been done on most common NACA airfoils and other streamline bodies to measure and enhance the aerodynamic characteristics under several flow conditions [Firooz and Gadami (2006) to Manoha et al. (2001)]. Huang et al. (2004) applied suction and blowing techniques on NACA 0012 to control flow separation. They revealed that perpendicular suction located at the leading edge increased lift coefficient better than other suction conditions and the location of tangential blowing at the trailing edge produced the maximum increase in the lift coefficient value. Yousefi et al. (2014) worked on the numerical optimization of suction jet parameters on the characteristics of NACA 0012. They concluded that suction located between 0.0175 and 0.125 of the chord length from the leading edge with 0.5 amplitude improved the aerodynamic characteristics of the airfoil; maximum increases in the lift, reduction in drag and stall improvement. Akcayoz and Tuncer (2009) worked on the maximization of lift to drag ratio through optimization of synthetic jet parameters on NACA 0015 airfoil in various angles of attack. Their results showed that the optimum jet location moved towards the leading edge, and as the angle of attack increased the optimum jet angle increased. Azim et al. (2015) delayed boundary layer separation through suction on NACA 4412 and optimized the suction parameter. They revealed that suction located 0.68 of the chord length, the suction pressure of 65kpa delay separation and the application of suction improved the lift to drag ratio approximately 2.24 times higher than that of without suction. The investigations have illustrated that suction located at an appropriate position modifies pressure distribution over an airfoil surface as such produce a satisfactory effect on lift and drag coefficients, hence mitigating the streamwise momentum loss in the growth of the separation thickness. In the current study, suction and length of the suction jet on aerodynamic characteristics of the NACA 23012 airfoil is numerically analysed at Reynolds number 3.4×10^6.

GOVERNING EQUATIONS

The fluid was modelled as a two dimensional, steady, turbulent and viscous incompressible flow with constant properties. The classical physics equations that governed the fluid dynamics for this study are the continuity and the momentum equations which are as follows.

$$\frac{\partial \overline{u_i}}{\partial x_i} = 0 \qquad (1)$$

$$\frac{\partial \left(\overline{u_i u_j}\right)}{\partial x_j} = -\frac{1}{\rho}\frac{\partial \overline{P}}{\partial x_i} + \frac{\partial}{\partial x_j}\left[v\frac{\partial \overline{u_i}}{\partial x_j} - \overline{u_i' u_j'}\right] \qquad (2)$$

where $\overline{u_i' u_j'}$ is the Reynolds stress tensor that incorporates the effects of turbulent fluctuations (Alfonsi, 2009).

THE TURBULENT MODEL

The turbulent model used to predict the mechanics of fluid and the behaviour of fluids around the airfoil is Menter shear stress transport two-equation model. The Menter shear stress two-equation model provides a great and excellent predictive capability for flow with separation. This model (kω-SST) includes k-ω and k-ε standard models as such it improves the calculation of the flow of the boundary layer with separation and removes the k-ω model sensitivity to external flow. The Menter shear stress model is presented as:

$$\frac{\partial}{\partial x_i}(\rho U_i k) = \widetilde{P_k} - \beta^* \rho k \omega + \frac{\partial}{\partial x_i}\left[(\mu + \sigma_k \mu_t)\frac{\partial k}{\partial x_i}\right] \tag{3}$$

$$\frac{\partial}{\partial x_i}(\rho U_i \omega) = \alpha \rho S^2 - \beta \rho \omega^2 + \frac{\partial}{\partial x_i}\left[(\mu + \sigma_\omega \mu_t)\frac{\partial \omega}{\partial x_i}\right] + 2(1 - F_1)\rho \sigma_{\omega 2}\frac{1}{\omega}\frac{\partial k}{\partial x_i}\frac{\partial \omega}{\partial x_i} \tag{4}$$

where β^* is 0.09 and $\sigma_{\omega 2}$ is 0.856. Away from the surface, the blending function is zero (k-e model). Inside the boundary layer, the blending function switches to unity (k-w model). $\widetilde{P_k}$, a production limiter was used in the SST model to prevent the buildup of turbulence in the stagnation regions(Menter, 1992) (Menter et al., 2003).

THE GEOMETRIC MODEL SELECTION OF PARAMETER

In this study, ANSYS FLUENT was used for the modelling and numerical simulation. Values for the Reynolds number and the free stream velocity was 3.4×10^6 and 49.66 m/s respectively. The geometry of NACA 23012 airfoil, suction jet location, suction jet angle and the jet length are shown in Figure 1. The chord length of the airfoil was 1 m; the suction jet length for this investigation was 2.5% of the chord length; the suction jet amplitude (i.e. the ratio of the suction jet velocity to free stream velocity) was between 0 and 0.3. Therefore, the following three parameters which are suction amplitude (A), dimensionless suction jet width $\left(H = \frac{h}{c}\right)$, suction jet location (L_j) were investigated for optimum performance of the NACA23012 wing. Since stall occurs on NACA 23012 at around 16^o AOA, the above investigations were carried out between 0^o – 18^o angles of attack. The jet entrance velocity components are defined as follows:

$$v = u_{jet}\sin(\theta + \beta) \tag{5}$$

$$u = u_{jet}\cos(\theta + \beta) \tag{6}$$

where β is the angle between the free-stream velocity direction and the local jet surface, and θ is the angle between the local jet surface and the jet output velocity direction. suction condition is represented with negative θ

NUMERICAL PROCEDURES

The second-order upwind scheme was employed to discretize the governing equations. In the simulations, second-order upwind discretization in space was used and then, the resulting system of equations was solved through Semi-Implicit Method For Pressure Linked Equations

(SIMPLE) procedure until a convergence criterion of O(5) reduction in all dependent residuals is satisfied. A C-type structured grid with multi-zone blocks was generated as a computational domain. The computational area was large enough to prevent the outer boundary from affecting the near flow field around the airfoil. The inlet and lower boundaries were fixed with a uniform inlet velocity value. The upper and outer boundary conditions were the free-stream boundaries that satisfy the Neumann condition. No-slip boundary condition was used on the aerofoil surface. A low free-stream turbulence intensity less than 0.15% was used to match the wind tunnel characteristics and the mesh of $y^+<1$ around the airfoil/ wing was ensured.

RESULTS AND DISCUSSION

Mesh Independent Study

The computations of the different sized grid were performed for NACA 23012 airfoil at Reynolds number 3.4×10^6 to ensure grid independency test to the calculated results through the study of lift and drag coefficients at the angle of attack 10^0, 12^0 and 16^0 for the fundamental conditions without the application of jet on the airfoil surface. Figure 1 presented the lift and drag indecency for lift and drag coefficient. The grid size with the fine mesh following a grid-independent result that produces a reasonable accuracy was selected to be 758410 cells.

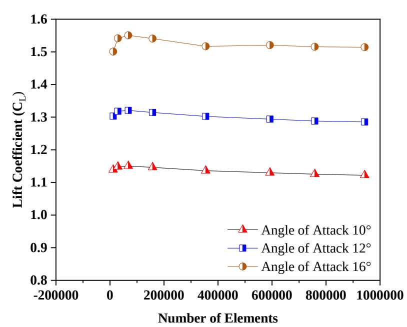

(a)

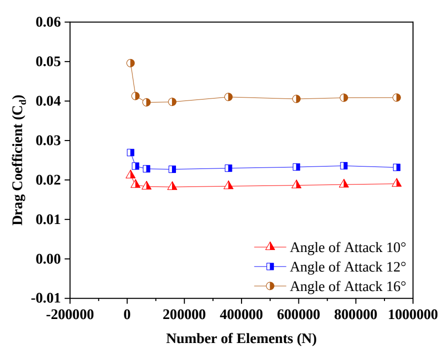

(b)

Figure 2: Mesh Indecency For (a) Lift Coefficient (b) Drag Coefficient

This mesh has a difference less than 0.001 from the preceding mesh as such the lift and drag ceased to have significant change as the number of quadrilateral elements increased as shown in details in Figure 1.

VALIDATION

For the validation of the data, the residuals in all simulations were continuing until the lift and drag coefficient reach a full convergence. The lift and drag coefficient were studied and compared with the experimental values of .Jacobs and Clay (1936). They investigated the Characteristics of the NACA 23012 airfoil under a Reynolds number of 3400000. The variation of the present work to the Jacob et al. experimental data started at the angle of attack of about 14^0 as shown in Figure 2. Thus, the percentage change between the present work and, Jacobs and Clay (1936) at an angle of attack 16^0 was 15.2%. The present computational results of lift coefficients show better agreement with Jacob et al. The significant variation is as a result of some uncertainty and the uncertainty could be attributed to several factors, such as different flow regimes, angles of attack, airfoil geometries, and turbulence model. Turbulence model selection has a significant effect on stall prediction and lift-to-drag ratio accuracy. The k-ω ST model has better stall prediction capability. For suction, the exact experimental data were not available.

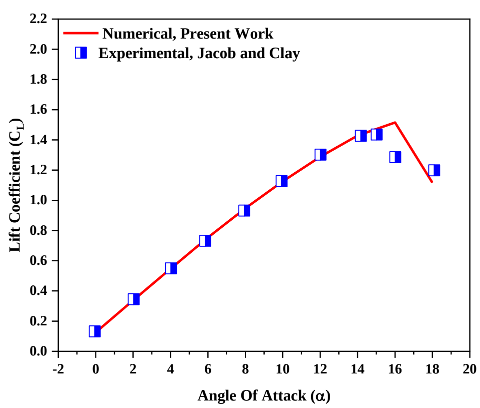

(a)

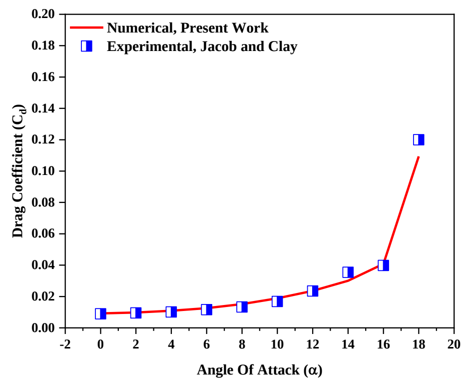

(b)

Figure 3: The comparison at Reynolds number 3.4×10^6 for (a) lift Coefficient (b) drag coefficient

Slot Selection

In enhancing the aerodynamic performance of suction, it is thereby necessary to place the suction in the appropriate position. The dependency of suction position on a various parameter such as Reynolds number, angle of attack (AOA), amplitude etc. makes the decision of choosing the best suction position complex because the parameters affect the position of suction. In other to ease the enormous complexities, the aerodynamic performance is measured at the various suction position on the upper surface of the aerofoil at amplitude 0.1 making Reynolds number and AOA constant at 3.4×10^6 and 10^o, 14^o, 18^o respectively as shown in detail in Figure 3. According to the velocity contour shown in detail in Figure 4, the trailing edge separation point is found around 0.148c from the leading edge of the aerofoil for aerofoil without suction at AOA 18^o. Suction slot close to the leading edge i.e. suction slot at 0.2c, moves the separation point more in the vicinity of the trailing edge, about 0.860c from the leading edge of the airfoil. On the contrary, the earlier suction slot such as 0.05c and suction slot towards the trailing edge such as 0.4c, 0.5c, 0.7c decreases the performance drastically as shown in detail in Figure 3 and Figure. 4. Therefore, the suction slot at 0.05c and 0.7c decreases the lift increases the turbulence and gives fully the adverse effect. This suggests that moving the slot downstream and upstream from 0.2c will produce a catastrophic separation as such the increase in turbulence causes the skin friction to contributes to the increase in drag coefficient than that of without suction and the lift also decreases slightly, hence, lift to drag ratio falls off drastically. But suction slot at 0.2c for AOA 14^o decreases the drag coefficient by 44.4% from 0.030 to 0.016 which results in 78.3% increase in the lift to drag ratio from that of without suction. So, therefore, for better aerodynamic performance, suction is done at slot 0.2c.

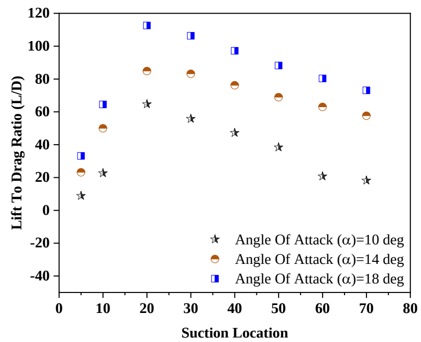

Figure 3: comparison between lift to drag ratio and suction location

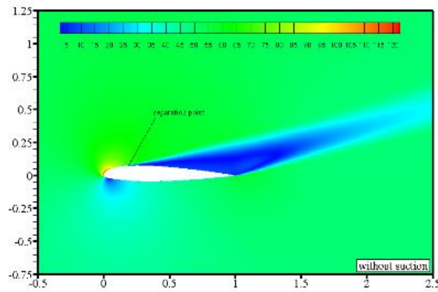

(a)

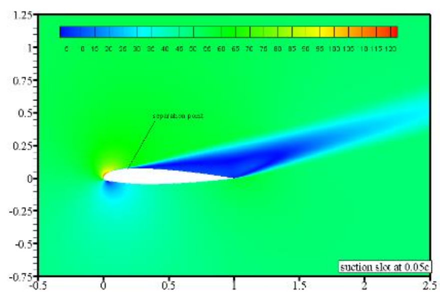

(b)

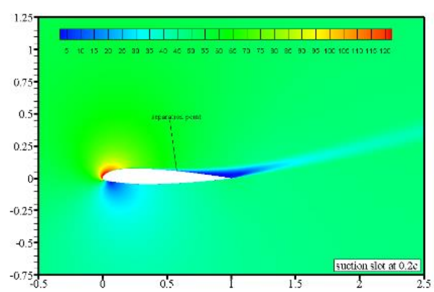

(c)

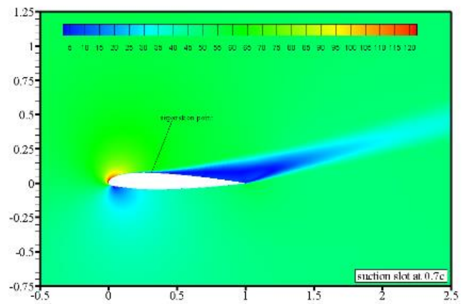

(d)

Figure 4: velocity contour for AOA= 18º (a) without suction; (b) with suction at slot 0.05c; (c) with suction at slot 0.2c and (d) with suction at slot 0.7c of the aerofoil at suction amplitude 0.1.

Effect of Suction Amplitude On Lift and Drag Coefficient

In Figure 5(a, and b) and Figure 6, the impact caused by the changes in suction amplitude was investigated. The location and width of the jet were fixed at 2.5% and 20% of the chord length, respectively. As suction amplitude was increased from 0.1 to 0.3 there was an improvement in the lift coefficient and reduction in the drag coefficient. However, the increase in the lift coefficient and reduction in drag coefficient are negligible for the angle of attack less than 10º for lift coefficient and angle of attack less than 4º for the drag coefficient. At an angle of attack of 18° with an amplitude of 0.3, the lift coefficient increased by 72.7%, and the drag coefficient decreased by 92.1%. However, increasing suction jet amplitude leads to improvement in the stall angle, which increased from 16º to 21.5º for jet amplitudes of 0 and 0.3, respectively. No suction conditions mean a jet amplitude of 0. Therefore, not only did the lift-to-drag ratio increases dramatically when suction was applied but also the stall angle was delayed effectively.

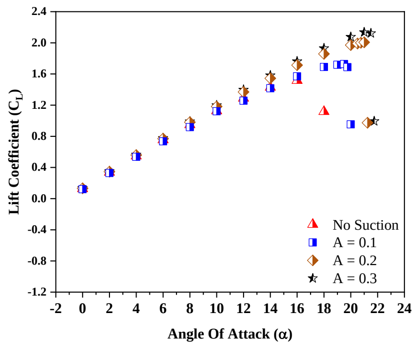

(a)

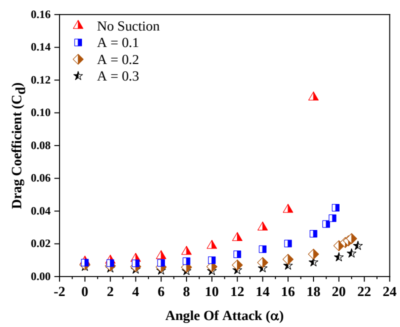

(b)

Figure 5: Comparison of (a)lift coefficient and (b)drag coefficient between suctioned aerofoil and un-suction aerofoil at a different angle of attack.

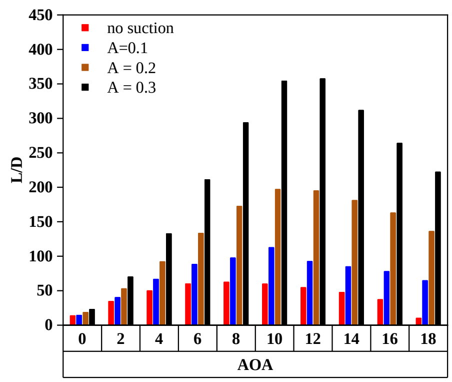

Figure 6: comparison of lift to drag ratio between suctioned and un-suction aerofoil at a different angle of attack

Trailing-Edge Separation for Different Suction Amplitude

The separation position moves towards the vicinity of the trailing edge of the aerofoil as the suction amplitude increase from 0.1 to 0.3. Initially, the introduction of the suction slot with an amplitude of 0.1 on the aerofoil moves the separation position towards the trailing edge in a great extent but later on; increase in suction amplitude moves the separation position slightly towards the trailing edge as shown in detail in Figure 7. For instance, at AOA=18^o., separation position moves from 0.148c to 0.526c of the airfoil when the suction amplitude of 0.1 was introduced on plain aerofoil and later on, when suction amplitude changes from 0.1 to 0.2 and from 0.2 to 0.3 the separation point moves from 0.526c to 0.860c and 0.860c to 0.895c respectively on the aerofoil. Changes in separation point from leading-edge with the increase in suction amplitude is shown in Figure. 7.

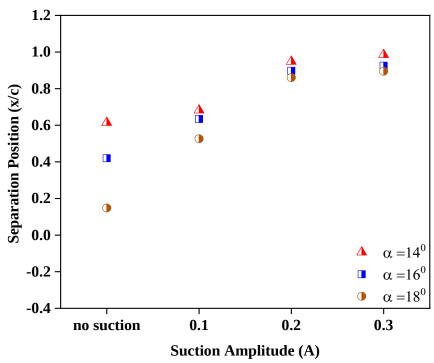

Figure 7: Change in trailing edge separation position with different suction amplitude.

CONCLUSION

In conclusion, the numerical investigation on the delay of catastrophic boundary layer separation over NACA 23012 airfoil has led to these remarks. The effects of suction parameters on a NACA 23012 airfoil for flow separation control were analyzed. Thus, employing numerical simulation, the results showed that the lift to drag ratio increased when suction amplitude was enhanced and the separation point moved to the vicinity of the trailing edge. The maximum lift to drag ratio value was obtained when suction amplitude reached 0.3. At the angle of attack 18^o and same suction amplitude, vortex behind the airfoil was eliminated entirely. Another significant point, as it has been described is that the flow separation control using suction had no significant influence on aerodynamic characteristics at low angles of attack. In addition, the use of suction on airfoil could raise the airfoil stall angle. In this investigation, the stall angle changed from 16 to 21.5^o when suction amplitude reached 0.3.

Finally, the airfoil lifts to drag ratio boost 75% and stall angle reached to 21.5^{o} at the suction amplitude of 0.3, the angle of attack 18^{o}, and 2.5 percent of the chord length as suction jet length.

REFERENCES

Akcayoz, E., and Tuncer, I. H. (2009). Numerical investigation of flow control over an airfoil using synthetic jets and its optimization. AIAC Paper 2009-043.

Alfonsi, G. (2009). Reynolds-Averaged Navier–Stokes Equations for Turbulence Modeling. Applied Mechanics Reviews, 62(4), 040802.

Azim, R., Hasan, M. M., and Ali, M. (2015). Numerical investigation on the delay of boundary layer separation by suction for NACA 4412. Procedia Engineering, 105(2014), pp. 329–334.

Bahatmaka, A., Kim, D.-J., Chrismianto, D., Setiawan, J. D., and Prabowo, A. R. (2017). Numerical investigation on the performance of ducted propeller. MATEC Web of Conferences. Reykjavík University.

Broeren, A. P., Addy, H. E., Bragg, M. B., and Busch, G. T. (2019). Aerodynamic Simulation of Ice Accretion on Airfoils.

Firooz, A., and Gadami, M. (2006). Turbulence Flow for NACA 4412 in Unbounded Flow and Ground Effect with Different Turbulence Models and Two Ground Conditions : Fixed and Moving Ground Conditions. Int. Conference on Boundary and Interior Layers (2006), pp. 1--11.

Gad -el_Hak, M. (2000). Passive. Cambrige University Press.

Geissler, W., and van der Wall, B. G. (2017). Dynamic stall control on flapping wing airfoils. Aerospace Science and Technology, 62, pp. 1–10.

Hand, B., Kelly, G., and Cashman, A. (2017). Numerical simulation of a vertical axis wind turbine airfoil experiencing dynamic stall at high Reynolds numbers. Computers and Fluids, 149, 12–30.

Huang, L., Huang, P. G., LeBeau, R. P., and Hauser, T. (2004). Numerical Study of Blowing and Suction Control Mechanism on NACA0012 Airfoil. Journal of Aircraft, 41(5), pp. 1005–1013.

Jacobs, E., and Clay, W. (1936). Characteristics of the NACA 23012 airfoil from tests in the full-scale and variable-density tunnels. Langley Field.

Jones, K., Dohring, C., and Platzer, M. (1996). Wake structures behind plunging airfoils - A comparison of numerical and experimental results. 34th Aerospace Sciences Meeting and Exhibit, (96), pp. 1–11.

Jones, L. E. (2008). Numerical studies of the flow around an airfoil at low Reynolds number. University of Southampton Faculty.

Kroll, N., Rossow, C., and Schwamborn, D. (2002). MEGAFLOW-a numerical flow simulation tool for transport aircraft design. ICAS Congress. Braunschweig.

Lee, S., and Bragg, M. B. (1999). Experimental Investigation of Simulated Large-Droplet Ice Shapes on Airfoil Aerodynamics Introduction. Journal of Aircraft, 36(5), pp. 844–850.

Lehmkuhl, O., Rodríguez, I., Baez, A., Oliva, A., (2013). On the large-eddy simulations for the flow around aerodynamic profiles using unstructured grids. Computers and Fluids, 84, pp. 176–189.

Lei, J., Zhao, S., and Wang, S. (2016). Numerical study of aerodynamic characteristics of FSW aircraft with different wing positions under supersonic condition. Chinese Journal of Aeronautics, 29(4), pp. 914–923.

Lu, L., Liu, M. ming, Teng, B., Cui, Z. dong, Tang, G. qiang, Zhao, M., and Cheng, L. (2014). Numerical investigation of fluid flow past circular cylinder with multiple control rods at low Reynolds number. Journal of Fluids and Structures, 48, pp. 235–259.

Manoha, E., Redonnet, S., Delahay, C., Sagaut, P., Mary, I., Ben Khelil, S., and Guillen, P. (2001). Numerical prediction of the unsteady flow and radiated noise from a 3D lifting airfoil. RTO AVT Symposium on “Ageing Mechanisms and Control: Part A - Developments in Computational Aero- and Hydro-Acoustics” (Vol. 079). Mancheste.

Menter, F. R. (1992). Improved Two-Equation Turbulence Models for Aerodynamic Flows. Moffett Field.

Menter, F. R., Kuntz, M., and Langtry, R. (2003). Ten Years of Industrial Experience with the SST Turbulence Model. In Turbulence Heat and Mass Transfer. Turkey: Heat and Mass Transfer, 4 (4), pp. 625–632.

Moriche, M., Flores, O., and García-Villalba, M. (2016). Three-dimensional instabilities in the wake of a flapping wing at low Reynolds number. International Journal of Heat and Fluid Flow, 62, pp. 44–55.

P. B. Makwana1. (2014). Numerical Simulation of Laminar Flow over Slotted Airfoil . IOSR Journal of Mechanical and Civil Engineering (IOSR-JMCE), 11(4), pp. 64–71.

Resendiz, C., and Cizmas, P. (2006). Control of flow separation by oscillatory fluid injection -

a numerical investigation. AandM University, Texas.

Schlichting, H. (1955). Free turbulent flows; jets and wakes. In Boundary Layer Theory (4th Edition, pp. 590–596). Mcgraw-Hill Book Company Inc.

Snorri Gudmundsson. (2013). General Aviation Aircraft Design : Applied Methods (1st Edition). Oxford: Butterworth-Heinemann.

Spentzos, A., Barakos, G. N., Badcock, K. J., Richards, B. E., Wernert, P., Schreck, S., and Raffel, M. (2005). Investigation of Three-Dimensional Dynamic Stall Using Computational Fluid Dynamics. AIAA Journal, 43(5), pp. 1023–1033.

Sunnyvale, C. and W. J. M. and P. K. (1984). Numerical Simulation of the Interaction of a Vortex with Stationary Airfoil in Transonic Flow. In AIAA 22nd Aerospace Sciences Meeting, pp. 1–27.

Yousefi, K., Saleh, R., and Zahedi, P. (2014). Numerical study of blowing and suction slot geometry optimization on NACA 0012 airfoil. Journal of Mechanical Science and Technology, 28(4), pp. 1297–1310.

NOMENCLATURE

α	airfoil angle of attack
α_{stall}	stalling angle of attack, coincident with the maximum lift coefficient
c	airfoil chord length drag coefficient
C_d	drag coefficient
C_L	lift coefficient
AOA	angle of attack
x/c	separation position
Re	Reynolds number based on chord surface length along with airfoil profile
L_j	suction width
A	suction jet amplitude
L_p	suction position
ρ	the density of the fluid
N	number of element
$\bar{P}$	the mean pressure
v	the kinematic viscosity
u_{jet}	the suction jet velocity

u_∞	the free stream velocity
$\bar{u}$	the mean velocity
$\overline{u_i' u_j'}$	the Reynolds stress tensor
F_1	the blending function
S	the invariant measure of the strain rate